Properties of pedestrians walking in line: Fundamental diagrams

Asja Jelić,[1,*] Cécile Appert-Rolland,[1,†] Samuel Lemercier,[2,‡] and Julien Pettré[2,§]
[1]*Laboratory of Theoretical Physics, CNRS (UMR 8627), University Paris-Sud, Batiment 210, F-91405 Orsay Cedex, France*
[2]*INRIA Rennes - Bretagne Atlantique, Campus de Beaulieu, F-35042 Rennes, France*
(Received 21 November 2011; published 28 March 2012)

We present experimental results obtained for a one-dimensional pedestrian flow using high precision motion capture. The full pedestrians' trajectories are obtained. In this paper, we focus on the fundamental diagram, and on the relation between the instantaneous velocity and spatial headway (distance to the predecessor). While the latter was found to be linear in previous experiments, we show that it is rather a piecewise linear behavior which is found if larger density ranges are covered. Indeed, our data clearly exhibits three distinct regimes in the behavior of pedestrians that follow each other. The transitions between these regimes occur at spatial headways of about 1.1 and 3 m, respectively. This finding could be useful for future modeling.

DOI: 10.1103/PhysRevE.85.036111 PACS number(s): 89.75.Fb, 89.65.−s, 89.40.Bb, 89.90.+n

I. INTRODUCTION

There is a growing interest to understand the behavior of pedestrians, not only in emergency regimes—which can represent a real danger for the persons involved—but also in normal pedestrians flows, for example, to improve the capacity of a pedestrian facility. But there is also a more fundamental interest for physicists to study pedestrian crowds, as these exhibit collective phenomena and show several types of pattern formation. Several models were proposed to describe the dynamics of pedestrians [1,2] which partially reproduce the behavior of real crowds. However, several intricate effects have to be taken into account, in particular, due to the bidimensional nature of pedestrian traffic (compared to the quasi-one-dimensional road traffic, for example). Pedestrians avoid each other by adapting both their velocity amplitude and direction [3,4]. It is tempting to separate these effects by considering some simplified configurations.

In particular, one-dimensional pedestrian flows allow one to restrict oneself to longitudinal interactions, and to avoid lateral ones. Such longitudinal interactions may occur in narrow corridors [5], where pedestrians cannot pass each other, or in larger corridors when the encounter of oppositely moving pedestrians induces the formation of several (possibly narrow) lanes [6,7]. The interpretation of two-dimensional data may require an understanding of the following behavior [8]. One-dimensional flows can be used to test the following behavior in models [9]. Besides, some models do use a decoupling between the angular and speed adaptation [3,10,11].

If the line on which pedestrians walk is closed, boundary effects are avoided, and it becomes easier to study the bulk behavior. Such experiments have indeed already been performed in the past. In Ref. [12], the distribution of time headways was measured. Seyfried *et al*. [13] have measured the density and velocity of pedestrians following an oval trajectory. They considered densities up to 2 ped/m, where ped means pedestrians, and were able to draw the corresponding fundamental diagram.[1] This experiment was compared to a similar one performed in India [14]. In both cases, data were obtained from localized measurements.

In this paper, we present new experimental results that were obtained on a circular path using high precision motion capture.[2] The trajectories of all pedestrians were reconstructed in three-dimensions for the whole duration of the experiments. As a result, we were able to obtain not only measurements that can be directly compared to previous studies, but we had access to new features.

In particular, we can now obtain an *instantaneous* fundamental diagram, giving the relation between the instantaneous velocity of a pedestrian and his instantaneous density, defined as the inverse of his spatial headway h. We show that such a fundamental diagram is a mixture between stationary behavior and transient behavior, for which the velocity does not have time to relax toward its stationary value. This may occur, for example, when a pedestrian arrives on the rear end of a jam, or on the contrary when it leaves the jam.

Our main result is that the behavior of pedestrians in a following regime exhibits two transitions, one occurring at a spatial headway of about 1.1 m and again another transition around 3 m. These transitions are clearly visible on the velocity–spatial-headway relation $v(h)$. Actually, this relation was found to be linear in previous experiments [13,14]. Our experiment has allowed us to access a much larger density range, and revealed that actually it is a piecewise linear relation.

We shall first describe the experiment in Sec. II. Experimental measurements of the fundamental diagram will be presented in Sec. III. We shall discuss in detail global, local (Sec. III A), and instantaneous fundamental diagrams (Sec. III B). In Sec. IV, we shall present our main result, showing that there exists two transitions in the behavior of pedestrians that can be seen in the velocity–spatial-headway relation $v(h)$. Our results will then be compared with

*asja.jelic@gmail.com
†cecile.appert-rolland@th.u-psud.fr
‡samuel.lemercier@inria.fr
§julien.pettre@inria.fr

[1]A fundamental diagram refers to a plot of either the velocity or the flux of some moving agents (pedestrians, cars, ants, ...) as a function of density.

[2]This experiment belongs to a series of experiments that was realized in the frame of the French PEDIGREE Project [15].

fundamental diagrams from other countries, in order to discuss possible cultural variations (Sec. IV B). We conclude in Sec. V.

II. THE EXPERIMENT

The goal of our experiment was to characterize one-dimensional pedestrian traffic at various densities. Different densities were obtained by modifying on the one hand the number of pedestrians involved, and on the other hand the path on which they walk.

Up to 28 pedestrians (20 males and 8 females) were involved in the experiment. The experiment was conducted inside a ring corridor formed by inner and outer circular walls of radii 2 and 4.5 m, respectively (see Fig. 1). Participants were told to walk in line along either the inner or outer wall, without passing each other. This resulted into two types of pedestrian trajectories: the inner circular path of observed average radius 2.4 and length 15.08 m, and the outer circular path of observed average radius 4.1 and length 25.76 m. Pedestrians were volunteers, and all were naive about the purpose of the experiment. They were asked to walk in a "natural way", as if they were walking alone in the street (and without talking to each other).

As a result of the variation of the number of pedestrians involved and of the use of the inner or outer circular path, the average density of pedestrians varied from 0.31 to 1.86 ped/m.

Table I gives a summary of the parameter values for which experiments were performed, and indicates the number of replicas that were performed for each parameter set. When it was possible (i.e., for low densities), replicas were involving different pedestrian sets. For half of the replicas, pedestrians were walking clockwise, and counterclockwise for the other half. The typical duration of an experiment was 1 min and somewhat more for higher densities.

The whole experiment was tracked by a VICON MX-40 motion capture system. Each pedestrian was equipped with 4 markers, one on the left shoulder, two on the right shoulder, and one on top of head. The experimental setting was surrounded by 12 infrared cameras able to detect the markers. The reconstruction software VICON IQ was used to convert the raw data into three-dimensional (3D) trajectories for each of the markers, with a frequency of 120 frames/s. The reconstruction is described in more details in Ref. [16]. From the position of the four markers, a mean position point is calculated for each pedestrian (we shall refer to this point as the "center of mass" of the pedestrian in the following, though it is more a mean position). Besides, in the analysis presented in this paper, we filtered out the step oscillations (steps characteristics will be studied in a next paper [17]).

TABLE I. Number of experimental replicas for each set of parameters (sorted by density): number of pedestrians, use of the inner or outer circular path, and density of pedestrians.

Number of pedestrians	Circle	Density (ped/m)	Number of replicas
8	Outer	0.31	8
16	Outer	0.62	6
24	Outer	0.93	4
16	Inner	1.06	8
28	Outer	1.09	5
20	Inner	1.32	5
21	Inner	1.39	4
24	Inner	1.59	8
28	Inner	1.86	4

In the data analysis, we had to take into account that some markers may be occluded at some times. Indeed it may happen that, due to the experimental setup, some markers are hidden by the walls or pedestrians' bodies. In particular for high densities, the markers on the shoulder closest to the wall were most of the time not visible. In the following analysis, we carefully checked to keep only data for which we had enough confidence.

III. FUNDAMENTAL DIAGRAM

The fundamental diagram, which gives flow or velocity as a function of density, is the main quantity that is usually measured in road or pedestrian systems. Indeed, it immediately shows transitions from free flow to jammed states. Besides, it allows for an easy comparison between different systems. It is

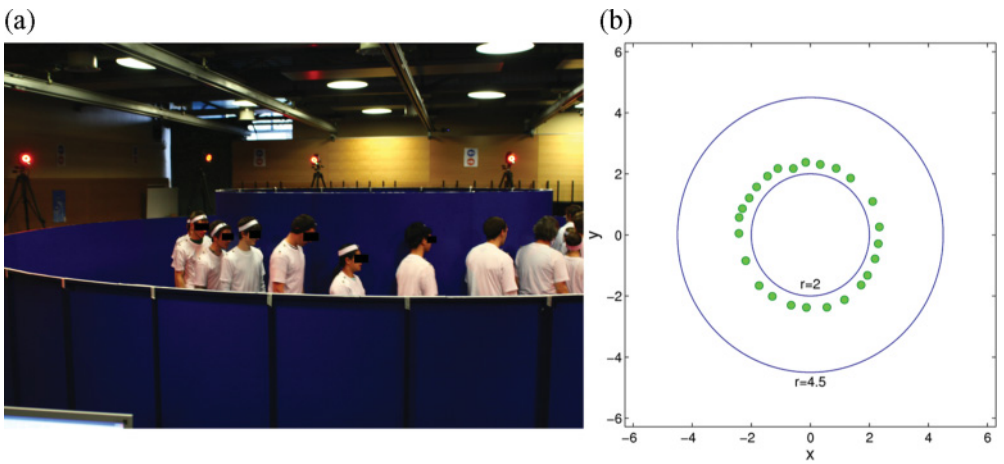

FIG. 1. (Color online) Experimental setup: (a) photograph of the experiment and (b) top view obtained through MATLAB treatment of the data, showing a snapshot of the pedestrians positions (small circles). Both images show an experiment along the inner circle.

also often used as a basic ingredient for modeling. But in fact, for pedestrians, the fundamental diagram was shown to vary significantly depending on the precise geometry within which pedestrians were walking [18,19].

Thus we shall compare our findings only with one-dimensional experiments, though it seems that comparisons with two-dimensional flows could be possible [13]. For previous one-dimensional experiments [13], measurements were performed locally on a window of the trajectory, and each data point was an average over this measurement window. With our data, at least three different definitions can be chosen for the density and velocity, depending on the way averages are performed, and ranging from global to instantaneous measurements.

(i) Global measurements: fluxes, velocities, and densities are averaged over the whole system and the whole duration of experiment (excluding the initial and final transients). Densities are thus discrete and correspond to the few densities imposed in the experiments. Both the average flux or average velocity can be plotted as a function of density.

(ii) Local measurements: velocities and densities are measured in a subpart of the system, and averaged over a finite time period. Local densities may vary around the global value. It is this type of measurements that can be compared to the experiments by Seyfried *et al*. [13,20]. As the way averages are performed may affect the shape of the fundamental diagram [21], we followed exactly the same procedure as in Ref. [13] to determine the local density and velocity, in order to allow for a direct comparison among experiments.

(iii) Instantaneous individual measurements: if the distance between two pedestrians is interpreted as the inverse of a density, then the instantaneous velocity of a given pedestrian can be plotted as a function of the inverse distance that is available in front of him.[3] This gives another type of fundamental diagram, which spans over a much larger range of densities, from 0.1 up to about 3 ped/m, as we shall see later.

A. Global and local fundamental diagrams

In this subsection, we present the results of the global and local measurements of the velocity as a function of density (Fig. 2), and compare them to the experiments by Seyfried *et al*. [13,20].

Measurement procedures

Note that in the case of global measurements, experiments with the same number of pedestrians do not necessarily correspond exactly to the same density. Indeed, global densities are calculated for each experiment by dividing a given number of participants N with the length of the circular path obtained using the measured average radius of all pedestrians during the whole duration t of the experiment. We denote this average

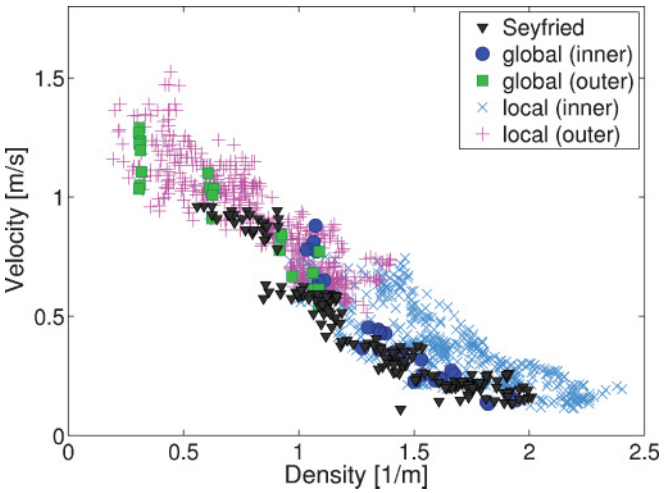

FIG. 2. (Color online) Fundamental diagram: Global and local measurements, compared with the measurements by Seyfried *et al*. [13,20]. Data were obtained either along the inner circular path (circle and 'x' symbols) or along the outer circular path (square and '+' symbols).

as $\langle\rangle_{N,t}$, so that

$$\rho = \frac{N}{2\pi \langle R\rangle_{N,t}}. \tag{1}$$

This procedure gives a small dispersion in the global values of density for experiments with the same number of pedestrians.

Measurement of the local velocity and density is performed by following the same procedure as in Ref. [13]. The local mean velocity and density are calculated by considering a segment $\Delta\theta$ of the circle as a measurement area. The velocity of each pedestrian j passing through this area is defined as the length $x = \Delta\theta\langle R\rangle_{N,t}$ divided by the time he or she needs to cross this circle area:

$$v_j = \frac{x}{t_j^o - t_j^i}, \tag{2}$$

where t_j^i and t_j^o are the in and out times at which a pedestrian j enters and exits the measurement area, respectively. Density of pedestrians inside the measurement area at time t is given by $\rho(t) = \sum_j \Theta_j(t)/x$, where $\Theta_j(t)$ is the fraction of space between pedestrian j and his follower $j+1$ that falls inside the measurement area

$$\Theta_j(t) = \begin{cases} \frac{t-t_j^i}{t_{j+1}^i - t_j^i} & \text{for} \quad t \in \left[t_j^i, t_{j+1}^i\right] \\ 1 & \text{for} \quad t \in \left[t_{j+1}^i, t_j^o\right] \\ \frac{t_{j+1}^o - t}{t_{j+1}^o - t_j^o} & \text{for} \quad t \in \left[t_j^o, t_{j+1}^o\right] \\ 0 & \text{otherwise.} \end{cases} \tag{3}$$

The density ρ_j for each person j is then calculated as $\rho_j = \langle\rho(t)\rangle_{\Delta t_j}$, i.e., as an average of the density in the measured area over the time interval $\Delta t_j = t_j^o - t_j^i$. Finally, in Fig. 2, for each density ρ_j, we plot the velocity v_j.

Discussion

Let us first consider the global fundamental diagram shown in Fig. 2. For similar densities, one notices a dispersion of the

[3]We neglect the thickness of people in these distance measurements, i.e., the distance that we consider is actually the distance between the centers of mass of successive pedestrians. Indeed we do not have any information about the real size of each pedestrian.

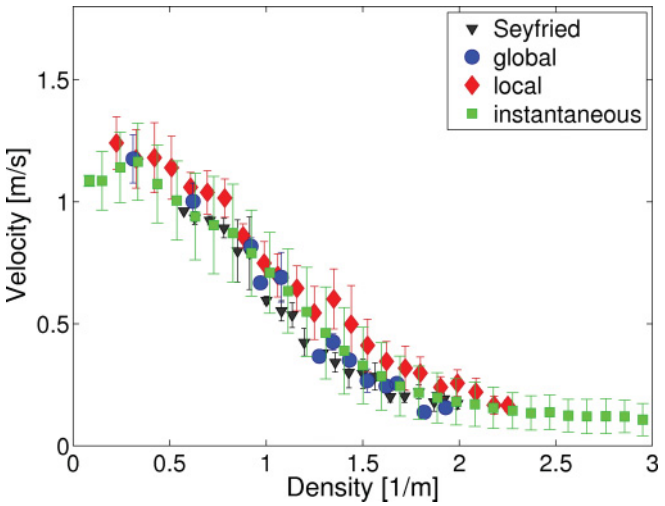

FIG. 3. (Color online) Fundamental diagram: results of the binning procedure applied to the global, local, and instantaneous measurements, as well as to the measurements by Seyfried *et al*. [13,20] Bars give the standard deviation.

global velocity values among different replicas. The dispersion is stronger for the lower densities. We explain this by the fact that at low densities, different individuals were involved in the various experimental replicas, therefore possibly imposing different preferred velocities. For higher densities, the same pedestrians could be part of several experimental replicas. Besides, global constraints restrict more the velocity choice of each pedestrian when density increases. As a result, dispersion is much lower for high densities. We see the same dispersion reduction on local data in Fig. 3, once a binning procedure has been applied.

Figure 2 shows that, as expected, the velocity decreases with increasing density. Actually, when the density increases, some stop-and-go waves are formed. It is possible with our experimental set-up to detect these waves very precisely [11,22]. A thorough study of such stop-and-go waves will be presented later.

In order to compare the fundamental diagram more easily than through data clouds, we have applied a binning procedure to the data, with the result shown in Fig. 3. Our results are in good qualitative agreement with Seyfried's [13], though the velocities that we find are systematically slightly above.

We find that our global and local measurements give quite close results as long as the density is smaller than 1.2 ped/m, while both measurements differ for larger densities, i.e., when stop-and-go waves arise.

B. Instantaneous fundamental diagram

As we have the full trajectories of all pedestrians at all times, we can also measure some "instantaneous" fundamental diagrams.

Measurement procedure

More precisely, for each pedestrian, at each time frame, we measure the instantaneous velocity and the distance h between the centers of mass of the pedestrian under consideration and his predecessor. We call this distance a "spatial headway," though it neglects the size of pedestrians. The inverse of this distance is interpreted as an instantaneous density.

Then, for a given pedestrian, these instantaneous density and velocity values are averaged over 60 consecutive time frames (i.e., over a time window of 0.5 s), generating one data point. The final fundamental diagram is obtained from the set of all the data points through a binning procedure.

Fundamental diagrams obtained from individual instantaneous measurements are given in Figs. 3, 4, and 6 and will be discussed below.

Influence of the number of detected markers

As discussed in Sec. II, at a given time frame some or all markers of a given pedestrian may be occluded. An interpolation is performed to generate data, but if the time window on which the markers are occluded is too long, the interpolation procedure may introduce some error in the inter-distance measurements, which results in unrealistic densities.

In the fundamental diagram of Fig. 4, we distinguish experimental data depending on which number of markers the measurement is based. More precisely, we define N_s as the minimum number of markers that were detected, at each of the

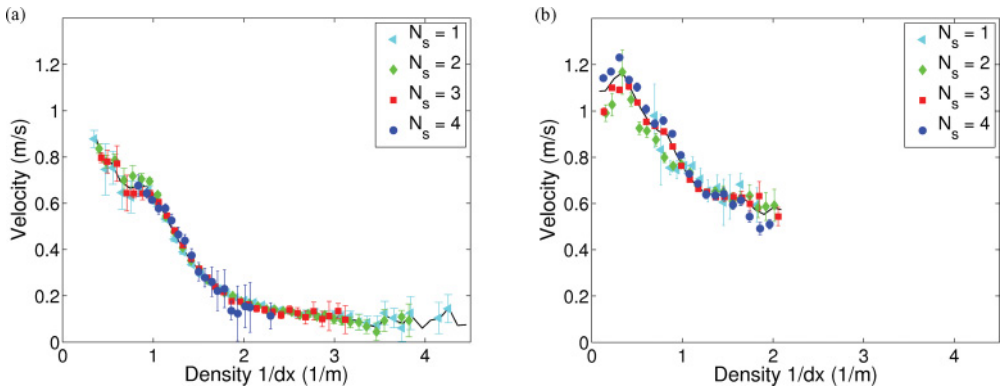

FIG. 4. (Color online) Fundamental diagram: Instantaneous velocity of individual pedestrians as a function of density, defined as the inverse of the instantaneous distance to the predecessor. Data are sorted by the minimal number of detected markers per pedestrian N_s for the (a) inner and (b) outer circular paths. We distinguish the cases $N_s = 1$ (cyan triangles), $N_s = 2$ (green diamonds), $N_s = 3$ (red squares), and $N_s = 4$ (blue circles). The solid line gives the average over all data, whatever the number of markers is. Error bars give the error on the mean.

consecutive 60 time frames over which we average, both for the observed pedestrian and his predecessor (with respect to which we determine the interdistance, i.e., inverse, density).

We have plotted these data on different plots [Figs. 4(a) or 4(b)] depending whether they were obtained on the inner or outer circular path, respectively.

We find that the data obtained for different numbers of markers mostly overlap. The main difference is that for low numbers of detected markers, the measured density reaches higher values. This seems to be an artifact of the measurements. Indeed, when there are only one or two markers that are detected for at least one of the pedestrians (predecessor or follower), then it is not obvious in most cases to decide whether these markers are on the head or on the shoulder. As the head markers are, on average, 10 cm ahead compared to shoulder markers, this creates an uncertainty on the distance between pedestrians, which should be of the order of 5 cm in the case of two detected markers (as at least one of them is on the shoulder), and 10 cm in the case of one marker. This uncertainty is negligible at low densities, but becomes relevant at high densities. In particular, it can explain why, on Fig. 4(a), data with one or two detected markers extend over densities up to 4.2 and 3.7 ped/m, respectively, while the maximum density measured with three detected markers is 3.1 ped/m: the uncertainty on position corresponds exactly (quantitatively) to this maximum density difference. As a consequence, we believe that the measurements beyond a density of 3.1 ped/m cannot be trusted.

In most cases, only three markers are detected. This is due to the walls along which pedestrians are walking. Figure 5 shows that on the outer circle, pedestrians that were detected with their four markers were on average walking at a larger distance from the wall than others. Indeed it is more difficult to detect the marker(s) on the wall's side when the pedestrian is very close to the wall. This is to be related to the fact that, for very low densities, the velocities of pedestrians with four markers are larger than those of pedestrians with three markers [see Fig. 4(b)].

No such effect is observed on the inner circle, for which there is no interest to escape from the wall, as it does not shorten the trajectory. As a result, much less data with four markers are available on the inner circle (about 10 to 20% at high densities when pedestrians are walking counterclockwise, and 5 to 10% when they are walking clockwise, i.e., when the shoulder equipped with two markers is close to the wall).

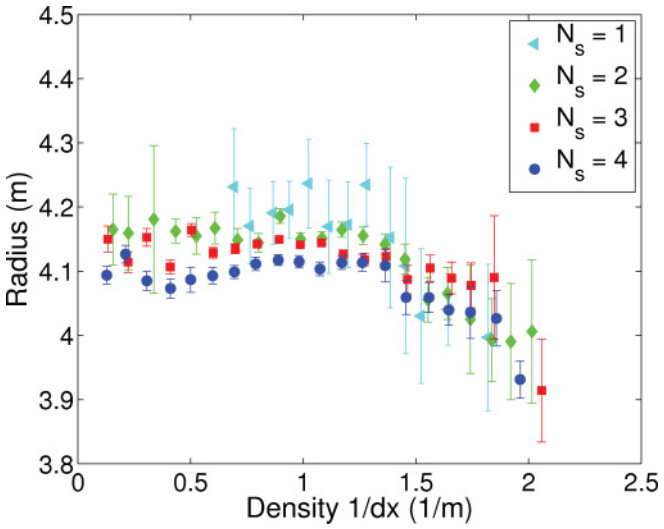

FIG. 5. (Color online) Radius as a function of the inverse spatial headway, for outer circle experiments. The plot is obtained as the result of a binning procedure over a large number of measurements. Each measurement corresponds to an average over 0.5 s, for one given pedestrian.

Discussion

Figure 5 also shows that for higher densities along the outer circle, pedestrians tend to walk at a slightly larger distance from the wall. This can be an attempt to increase their visual horizon, and also to limit the consequences of coming too close to a collision with the predecessor. Again, this effect is not present on the inner circle, probably because pedestrians are more reluctant to escape from the wall, as it lengthens their trajectory.

In Fig. 6, we superimpose the fundamental diagrams obtained for the inner and outer circular paths. The discrepancies that seem to arise do not actually indicate significant differences in the behavior of pedestrians, and we shall see below that they can be easily interpreted. The average over all data (inner and outer circles) goes smoothly over the whole density range.

The vertical line indicates the maximal (minimal) global density obtained on the outer (inner) circle (which are, respectively, 1.09 and 1.06 ped/m, as indicated in Table I). This means that data corresponding to the inner circle that are on the left of this vertical line correspond to densities that are far from average, i.e. they can be observed only if there are strong fluctuations of the density. When such a fluctuation

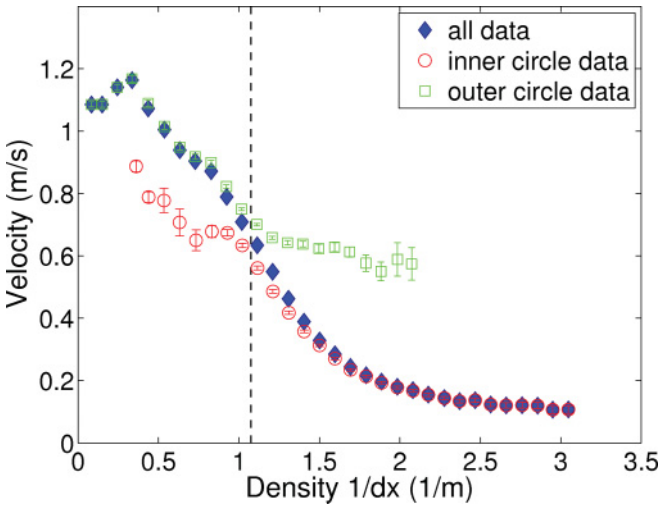

FIG. 6. (Color online) Fundamental diagram: Instantaneous velocity of individual pedestrians as a function of density, defined as the inverse of the instantaneous spatial headway to the predecessor. Data corresponding to the inner (outer) circle are plotted with red circles (green squares), while the average over all data is plotted with blue diamonds. The vertical line indicates the maximal (minimal) global density obtained on the outer (inner) circle (1.09 and 1.06 ped/m, respectively). Error bars give the error on the mean.

toward low density occurs, a pedestrian suddenly has a larger spatial headway. Because he has a nonvanishing reaction time and a finite acceleration, he will adapt his velocity to this new situation with some delay. It is also possible that the pedestrian has enough information to anticipate that this fluctuation of the spatial headway will be short lived and thus to decide not to adapt to it. In both cases, as a result, his velocity will be lower than it would be in a stationary state. This is what we observe: the values coming from the inner circle data that are on the left of the vertical line correspond to lower velocity values. This should not be an effect of the geometry but rather the sign that the velocity has not fully relaxed to its stationary value for these data. Since these fluctuations in density are rather rare events, these points have a low weight if we take the average over all data: the average coincides with the outer circle values.

In a similar way, on the right of the vertical line, the average over all data coincides with the inner circle data. Large densities can be observed on the outer circle only if there are density fluctuations. Again, a pedestrian submitted to a fluctuation of his spatial headway toward small distances will not react immediately, and as a result the velocity corresponding to these fluctuations will be higher than in the stationary state. This effect may here be enhanced by the fact that, on the outer circle, the pedestrians can see quite far ahead. The pedestrian can all the more anticipate that his predecessor will accelerate again and thus accept to come closer to him without decreasing much his own velocity. Indeed, the decrease in the radius that was observed in Fig. 5 occurs precisely in a density range from 1.2 to 2 ped/m, i.e., a density range corresponding to transient fluctuations (as these densities are above the global density). This can be related, as mentioned earlier, to a strategy to see further ahead and to limit the inconvenience of coming very close to the predecessor. Such a strategy is not so interesting on the inner circle, as an increase in the radius does not improve so much the visual field, and does not shorten the trajectory.

Thus we can explain the branches going away from the average behavior on Fig. 6 as being a signature of transient behaviors, when pedestrians' velocities do not have time to relax toward their stationary value. Besides, the weight of such transients is low compared to the remaining set of data.

The velocity-density points averaged on all data (blue diamond symbols on Fig. 6) show no discontinuity when going from the outer to the inner circle data.

The fundamental diagram averages over both stationary and transient behaviors, which cannot be easily separated. For low global densities, though fluctuations may arise from individual variations in the walking speed, the distribution of pedestrians is more or less homogeneous along the circle. When the global density becomes quite high, stop-and-go waves are produced. The maximal global density on the inner circle is 1.86 ped/m. Thus densities larger than this value are only obtained within compression waves. However, jams are quite stable, and even if there are some transient behaviors when people enter or leave the jam, inside the jam we would *a priori* consider that pedestrians are in a stationary state, i.e., that they have adjusted their velocity to the space available in front of them.

We have plotted the obtained averaged fundamental diagram together with the fundamental diagrams from the global and local measurements in Fig. 3. It is remarkable that even at densities as large as 3 ped/m, the velocity does not vanish but rather reaches a limiting value. This is consistent with other observations in two-dimensional flows showing that, in contrast with car traffic, pedestrians can move on even at very high densities [23].

IV. PHASE TRANSITIONS IN THE FOLLOWING BEHAVIOR

A. Experimental evidence of three dynamical regimes

In Ref. [13], Seyfried *et al*. have observed that the velocity of individuals is related to the spatial headway (distance to the predecessor) by a linear relation. With our experimental data, we are able to cover a larger range of velocities (or, equivalently, of instantaneous densities) and we find that

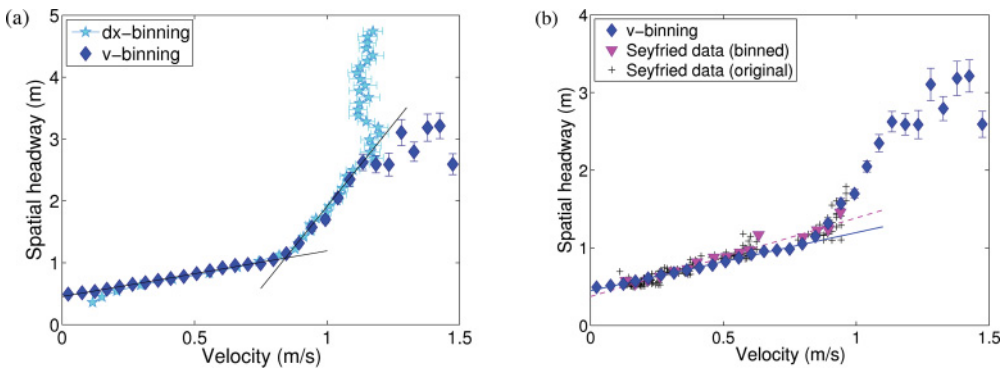

FIG. 7. (Color online) Spatial headway $h = 1/\rho$ as a function of velocity v. Each figure is obtained as the result of a binning procedure over a large number of measurements. Each measurement corresponds to an average over 0.5 s, for one given pedestrian. On (a), experimental data are plotted using both a horizontal (cyan stars) and a vertical (blue diamonds) binning procedure. Indeed, a binning on spatial headway values is more appropriate when the velocity saturates. Solid lines are fits of the data in the strongly and weakly constrained regimes. On (b), our data (blue diamonds) are compared with the measurements obtained in Ref. [13] (magenta triangles). The lines (respectively, solid-blue and dashed-magenta) correspond to fits of our data and Seyfried's data, both restricted to a velocity <0.8 m/s.

TABLE II. Adaptation time (or sensitivity) in the three regimes. Each adaptation time is obtained from a linear fit of the spatial headway–velocity relation in Fig. 7(a). For the free regime we fitted data with interdistance $h > 3.2$ m. However, as the curve is almost vertical and statistical errors obviously large, the numerical value is not meaningful; we can just conclude that the velocity saturates for these spatial headways.

Regime type	Adaptation time (s)
Free	13.7
Weakly constrained	5.32
Strongly constrained	0.74

there are actually several linear regimes, with different slopes [Fig. 7(a)].[4]

Three regimes can clearly be distinguished:

(a) For spatial headways greater than 3 m, pedestrians walk with their preferred velocity and do not seem to interact much with other pedestrians. Thus we call this state *free* regime.

(b) For spatial headways between 1.1 and 3 m, the velocity depends only weakly on the interdistance, and pedestrians do not slow down much. We shall refer to this regime as *weakly constrained*.

(c) For spatial headways below 1.1 m (or equivalently, instantaneous densities greater than 0.9 ped/m), the adaptation of the velocity to the spatial headway is much more pronounced. We shall refer to this regime as the *strongly constrained* regime.

The crossover between weakly and strongly constrained regimes occurs for a velocity around 0.8 m/s.

Surprisingly, the adaptation in the strongly constrained regime follows the same linear law even when the velocity comes very close to zero.

When the velocity tends to zero, pedestrians remain at a certain minimal distance h_0 from each other. It must be remembered that the spatial headway is here defined between centers of mass, while pedestrians have a certain thickness.

The slope in each linear regime has the dimension of time. Following [13], we interpret it as a sensitivity to the spatial headway. It describes how strongly the pedestrian adapts his velocity to the available space in front of him. It can also be seen as an adaptation time, as it is the time available to react before being at the minimal distance h_0 from the current position of the predecessor.

It is natural that the adaptation time decreases when the spatial headway decreases, as possible collisions are more imminent. The surprise here comes from the fact that the characteristic adaptation time does not vary smoothly but only takes three values with sharp transitions between them. Table II summarizes the values of the adaptation time in the three regimes.

[4]When a binning on velocity is used, it is not possible to observe the saturation of the velocity at low densities. The vertical part of the relation shown in Fig. 7(a) can be seen only with a binning on the spatial headway, while for the almost horizontal part at low densities, a binning on the velocity is more appropriate. Thus we superimpose the results obtained for both types of aggregating procedures.

TABLE III. Slope (adaptation time) and intercept with the zero velocity axis (minimal distance h_0) of a linear fit of the distance-headway–velocity relation in the strongly constrained regime. The French and corrected German values were obtained from a linear fit over not-binned (original) data for velocities smaller than 0.8 m/s in Fig. 7(b). We indicate the values published in Ref. [14] in parentheses.

	France	Germany	India
Intercept a (m)	0.45	0.37 (0.36)	(0.22)
Slope b (s)	0.75	1.01 (1.04)	(0.89)

B. Comparison of fundamental diagrams from different cultures

A comparison between data obtained in Germany and India [14] showed that walking characteristics could be culturally dependent. Before comparing our French data to those, it should be noticed on Fig. 7(b) that the beginning of the weakly constrained regime was already visible in the case of Seyfried's data [13], and that, interestingly enough, the transition occurs around the same velocity as for the French data.

When measuring the slope for the strongly constrained regime, one should be careful not to include data from the weakly constrained regime. However, though this was not taken into account in Ref. [13], the difference with the new slope that we have measured from their data is small (see Table III). There is still some uncertainty on the slope for the German data, as there are not too many data for $v > 0.6$ m/s. Besides, it seems that there was a large statistical fluctuation around a velocity of 0.6 m/s [see Seyfried's data in Fig. 7(b)] which may bias the result.

Still, it seems that for a given spatial headway, velocities are systematically slightly higher in the French case than in the German case. Also, a higher intercept value h_0, which can be seen as a minimal personal space [14], is observed in the French data. A high intercept means that pedestrians do not accept too small distances even in strong jamming. Consistent with these two facts, the French adaptation time is smaller than the German one, which means that their reaction at small distances is stronger.

Finally, for Indian data, we were not able to check whether the linear fit was performed only on the strongly constrained data. From the available values for the slope and the intercept of the linear fit performed in Ref. [14], we can conclude that the minimal personal space takes the lowest value for Indian pedestrians, while their adaptation time to the change of spatial headway is in between the French and the German values.

To say it otherwise, in view of the current available data, we could say that the strategy of Indian pedestrians facing jamming is rather to accept small distances, the strategy of French pedestrians is rather to break hard, and the strategy of German pedestrians is to walk at lower velocities.

However, it should be underlined that these cultural differences are weak, and that remarkably, in the three countries considered, velocity varies linearly with distance for distances below one meter. There seems to be a kind of universality in pedestrian's behavior, that would be interesting to probe on a larger range of densities.

V. CONCLUSION

In this paper, we present some analysis of new experiments for pedestrians walking on a line using high precision motion capture. We have focused on the fundamental diagram measurements and shown that various definitions for the velocity and the density could be used, bringing complementary information. In particular, our data allowed a measurement of the instantaneous fundamental diagram. We have shown that such a fundamental diagram actually aggregates both stationary and nonstationary behavior. Indeed, for a given experiment, the results obtained far from the global density, i.e., for fluctuations, show quite a different behavior from the average behavior, as the velocity is for a while not adapted to the available space—a feature that can be seen as fluctuations around the mean behavior in the fundamental diagram.

Our main result is to show that the velocity–spatial-headway relation allows us to distinguish three linear regimes, that we call free, weakly constrained, and strongly constrained. The crossovers between these regimes are quite sharp. The sensitivity, or adaptation time, characterizes how strongly a pedestrian adapts his velocity to the space available in front of him. Instead of changing continuously, the adaptation time takes only three discrete values, corresponding to the three regimes. This observation should give new directions for further modeling.

Any comparison between different sets of data should be careful at covering enough densities to distinguish these various regimes. Here we have compared our French data obtained in the strongly constrained regime with German [13] and Indian [14] data. When facing congestion, a pedestrian can choose to slow down preventively, or to react more rapidly to changes, or to accept smaller distances with his predecessor. Cultural background can enhance one of these strategies, though further careful experiments would be needed to confirm the trends that we observe. However, cultural effects are on the whole rather weak, and pedestrians' behavior appears mostly universal at the small distances for which a comparison could be made. Further studies covering a larger density range would be of interest, in particular to explore the robustness of the transitions that we have found.

A thorough study of the stepping behavior of pedestrians, depending on the density and velocity, will be published in a future paper [17].

In a separate paper, an analysis of the following behavior of pedestrians has led to the development of a microscopic model, which is shown to reproduce quite well the stop-and-go waves observed in the experiment [11,24]. Besides, its extension to a quasi-1D multilane model to simulate unidirectional flow in a corridor turns out to give results as realistic as alternative methods [11].

ACKNOWLEDGMENTS

This work has been supported by the French "Agence Nationale pour la Recherche (ANR)" in the frame of the Contract "PEDIGREE" (Contract No. ANR-08-SYSC-015-01). The PEDIGREE Project is financed by the French ANR and involves four research teams in Rennes (INRIA), Toulouse (IMT, CRCA), and Orsay (LPT).

Experiments were organized and realized by the PEDIGREE partnership [15] at University Rennes 1, with the help of the laboratory M2S from Rennes 2. We are in particular grateful to Armel Crétual, Richard Kulpa, Antoine Marin, and Anne-Hélène Olivier for their help during the experiments. A.J. acknowledges support from the RTRA Triangle de la physique (Project 2011-033T).

[1] D. Helbing and P. Molnár, Phys. Rev. E **51**, 4282 (1995).
[2] C. Burstedde, K. Klauck, A. Schadschneider, and J. Zittartz, Physica A **295**, 507 (2001).
[3] J. Ondrej, J. Pettré, A.-H. Olivier, and S. Donikian, ACM Trans. Graphics **29**, 123 (2010).
[4] S. Paris, J. Pettré, and S. Donikian, Comput. Graphics Forum-Eurographics **26**, 665 (2007).
[5] M. Chraibi, A. Seyfried, and A. Schadschneider, Phys. Rev. E **82**, 046111 (2010).
[6] M. Moussaïd, E. Guillot, M. Moreau, J. Fehrenbach, O. Chabiron, S. Lemercier, J. Pettré, C. Appert-Rolland, P. Degond, and G. Theraulaz, PLoS Comput. Biol. (to be published).
[7] J. Zhang, W. Klingsch, A. Schadschneider, and A. Seyfried, J. Stat. Mech. (2012) P02002.
[8] A. Johansson, Phys. Rev. E **80**, 026120 (2009).
[9] A. Seyfried, B. Steffen, and T. Lippert, Physica A **368**, 232 (2006).
[10] M. Moussaïd, D. Helbing, and G. Theraulaz, Proc. Nat. Acad. Sci USA **108**, 6884 (2011).
[11] S. Lemercier, A. Jelic, R. Kulpa, J. Hua, J. Fehrenbach, P. Degond, C. Appert-Rolland, S. Donikian, and J. Pettré, Comput. Graphics Forum-Eurographics (to be published).
[12] D. Jezbera, D. Kordek, J. Kříž, P. Šeba, and P. Šroll, J. Stat. Mech. (2010) L01001.
[13] A. Seyfried, B. Steffen, W. Klingsch, and M. Boltes, J. Stat. Mech. (2005) P10002.
[14] U. Chattaraj, A. Seyfried, and P. Chakroborty, Adv. Complex Syst. **12**, 393 (2009).
[15] More information can be found at http://www.pedigree-project.info.
[16] S. Lemercier, M. Moreau, M. Moussaïd, G. Theraulaz, S. Donikian, and J. Pettré, Lect. Notes Comput. Sci. **7060**, 365 (2011).
[17] A. Jelić, S. Lemercier, C. Appert-Rolland, and J. Pettré, Report (unpublished).
[18] J. Zhang, W. Klingsch, A. Schadschneider, and A. Seyfried, J. Stat. Mech. (2011) P06004.
[19] W. Daamen and S. P. Hoogendoorn, Transp. Res. Rec. **1828**, 20 (2003).

[20] A. Seyfried, B. Steffen, W. Klingsch, T. Lippert, and M. Boltes, in *Pedestrian and Evacuation Dynamics 2005*, edited by N. Waldau, P. Gattermann, H. Knoflacher, and M. Schreckenberg (Springer, Berlin, 2007).

[21] A. Schadschneider and A. Seyfried, Networks Heterog. Media **6**, 545 (2011).

[22] S. Lemercier, A. Jelic, J. Hua, J. Fehrenbach, P. Degond, C. Appert-Rolland, S. Donikian, and J. Pettré, Revue Électronique Francophone d'Informatique Graphique **5**, 67 (2011).

[23] D. Helbing, A. Johansson, and H. Z. Al-Abideen, Phys. Rev. E **75**, 046109 (2007).

[24] J. Hua, J. Fehrenbach, S. Lemercier, A. Jelic, C. Appert-Rolland, S. Donikian, J. Pettré, and P. Degond, Report (unpublished).